A new scheme for lidar Doppler detection on the intermediate frequency at increased laser instability

D. V. Stoyanov, B. M. Bratanov, and M. D. Angelova
Institute of Electronics, Bulgarian Academy of Sciences, 72 Lenin Boulevard, 1784 Sofia, Bulgaria

(Received 5 March 1991; accepted for publication 28 July 1991)

A new scheme for Doppler lidar detection by frequency shifted tracking of the reference frequency is described. The main advantages of the scheme are wide tolerable range of the laser instabilities (in principle more than 100 MHz), easy wideband tuning of the tracking frequency, one analog output by A/D converter with a sampling rate of only several times higher then the maximum expected Doppler frequency. It is shown how to account for the chirp history. The use of frequency synthesis for Doppler detection in wide frequency band of laser instabilities is considered.

I. INTRODUCTION

The accuracy of Doppler lidars is strongly affected by the instabilities of laser sources. To realize a relative error of 1 m/s, the frequency stability must be better than 10^{-9} (or $\approx$100 kHz at $\lambda = 10\,\mu$m). At higher fluctuation bandwidth $\Delta\omega_0$ of the reference intermediate frequency ω_0, serious problems arise in the detection system, such as accurate tuning of the coherent oscillator in wide frequency range, especially for airborne and space borne lidars; the effect of frequency dependence of the 90° phase shifter in the quadrature detector on the determination of the velocity direction, etc. Two analog-digital converters (ADC) for the inphase and quadrature channels are usually used.[1-3]

In this article a new scheme for Doppler detection at the intermediate frequency, based on the tracking heterodyne,[4,5] is described. The main advantages of the method are wide tolerable range of the laser transmitter instabilities (in principle more than 100 MHz), easy wideband tuning of the tracking heterodyne, one analog output by ADC with a sampling rate of only several times higher than the maximum expected Doppler frequency. It is shown how to account for the chirp effect of the emitted pulse. The proposed method may be used in the infrared coherent lidars at $\lambda = 10.6\,\mu$m with increased frequency instabilities 10^{-6}–10^{-7}.

II. DESCRIPTION OF THE METHOD

The block schematic of the Doppler detector is shown in Fig. 1(a) as a part of the lidar system. The hybrid TE CO_2 laser transmitter is assumed. The backscattered signal

$$A_s(t) = a_s(t)\cos(\omega_0 + \omega_D)t \tag{1}$$

is extracted by the optical mixing on the photodiode PD-1, where $A_s(t)$ is the amplitude; ω_D is the Doppler shift, $\omega_D < \omega_{Dm}$, ω_{Dm} is the maximum expected Doppler shift.

There are two reference channels in the lidar scheme. The reference signal of an intermediate frequency $\omega_0 = |\omega_{cw} - \omega_{LO}|$ is formed by the photodiode PD-2 before the emitted pulse, mixing the radiations of the local oscillator (LO) (frequency ω_{LO}) and the continuous-wave laser (frequency ω_{cw}) of the hybrid laser. Coherent detection of the emitted pulse is provided by the second reference channel of the photodiode PD-3. The return signal $A_s(t)$ and the emitted pulse signal $A_p(t)$ are fed through the multiplexer (MP) to the Doppler detector [inside the dashed contour on Fig. 1(a)] described here. The synchronization of the lidar is provided by the control block, according to the timing diagrams on Fig. 1(b).

The reference signal $A_0(t) = a_0\cos(\omega_0 t)$ by PD-2 is fed to the frequency-voltage transformer 1, gated by the pulse τ_1 of the control block. The output voltage, proportional to the reference frequency ω_0 is fed into the voltage-controlled oscillator (VCO). Let the input reference frequency ω_0 fluctuates within the range $\Delta\omega_0 = \omega_h - \omega_l$, where $\bar{\omega}_0 = (\omega_h - \omega_l)/2$. $\bar{\omega}_0$ is the mean-reference frequency, ω_l and ω_h are the lower and higher frequency extrema, respectively. The frequency ω_v of the VCO is tuned to be shifted in respect to reference frequency ω_0, satisfying the simple conditions: $\omega_v = \omega_0 + \Omega(\omega_0)$, $\Omega_{min} > \omega_{Dm}$ (where Ω_{min} and Ω_{max} are respectively the minimum and the maximum frequency differences), when ω_0 fluctuates within the bandwidth $\Delta\omega_0$. The function $\Omega(\omega_0)$ is assumed arbitrary. This is shown in Fig. 2, where the measured curve $\omega_v(\omega_0)$ used in the testing is presented. Thus, the frequency ω_v of the VCO will track closely the fluctuating reference frequency ω_0. The reference signal $A_0(t)$ and the signal of VCO $A_v(t) = a_0\cos\omega_v t$ are used by the block 3 to measure $\Omega(\omega_0)$ during the pulse τ_2 and to store it before the TE pulse arrival.

Passage of the TE pulse momentarily quenches the lasing of cw laser[6,7] and thus the reference signal is not available by PD-2 during the receiving of lidar backscattered signals. This function is carried out by the VCO. The two oscillations $A_s(t)$ and $A_v(t)$ are mixed in block 4. The spectrum $S(\omega)$ of the mixed signals (Fig. 3) contains two well-separated signal bandwidths: the first one is around the frequency $\Omega(\omega_0)$ and the second one is around $2\omega_0 + \Omega(\omega_0)$. The low-frequency edge ω_l of the fluctuation bandwidth $\Delta\omega_0$ may be tuned to satisfy the condition $\omega_l \approx 3\Omega_{max}$. Now using a lowpass filter 5 with cutoff frequency $\approx 2\Omega_{max}$, the useful Doppler signal $B_s(t)$ within the lower band of the spectrum $S(\omega)$ may be easily extracted:

$$B_s(t) \approx a_s(t)a_0\cos[\Omega(\omega_0) - \omega_D]t. \tag{2}$$

 0034-6748/91/122940-04$02.00

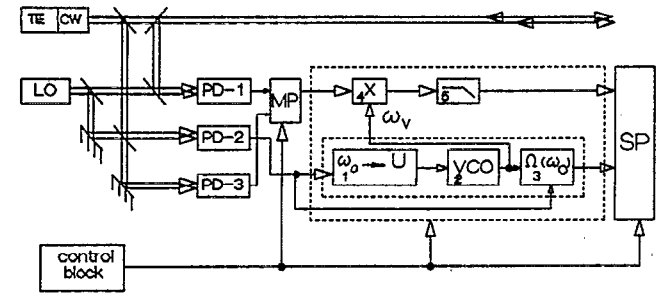

(a)

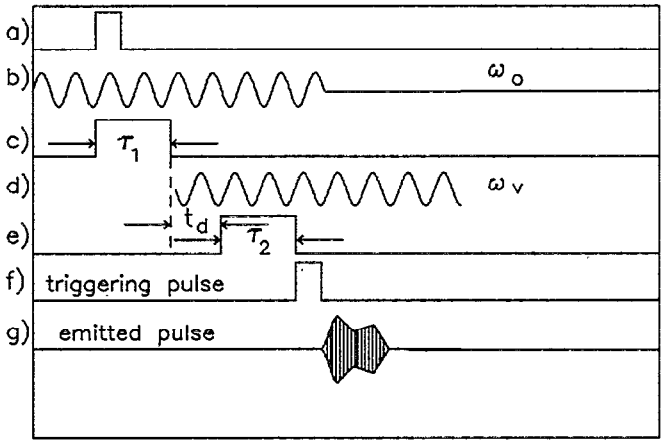

(b)

FIG. 1. (a) Doppler detection scheme (inside the dashed contour) as a part of the lidar system scheme: 1—frequency-voltage transformer, 2—voltage-controlled oscillator of frequency ω_v, 3—measuring scheme of the frequency difference $\Omega(\omega_0)$, 4—Doppler mixer, 5—low-pass filter, TE—pulse CO_2 laser, CW—continuous-wave laser, LO—local oscillator, PD-1—optical mixer for the backscattered flux, PD-2—reference optical mixer for the cw and LO lasers, PD-3—reference optical mixer for coherent detection of the transmitter TE pulse, SP—Doppler signal processor, MP—multiplexer. (b) Timing diagram of the lidar operation: a—starting pulse, b—reference intermediate signal of frequency ω_0 by the PD-2 mixer, c—pulse τ_1 for measuring the reference frequency, d—reference signal of frequency ω_v by VCO, e—pulse τ_2 of delay t_d for measuring the frequency difference $\Omega(\omega_0)$, f—triggering pulse for the TE laser, g—TE-laser pulse.

Therefore, for an arbitrary walk of the reference frequency ω_0 within the bandwidth $\Delta\omega_0$, the Doppler spectrum of $B_s(t)$ is localized in a well-isolated, stable bandwidth $0\text{–}2\Omega_{max}$. The signal $B_s(t)$ contains the entire

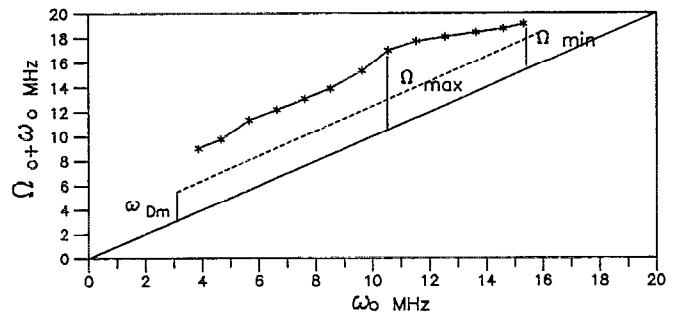

FIG. 2. Graph of the tracking frequency $\omega_v(\omega_0)$ by VCO, following approximately the fluctuations of the reference frequency ω_0 by a preliminary measured shift $\Omega(\omega_0)$.

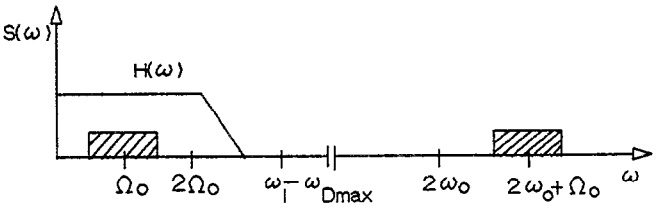

FIG. 3. Spectrum of the signal output by the Doppler mixer 4 in Fig. 1, [$H(\omega)$ is the transfer function of the low-pass filter].

Doppler spectrum and may be sampled by one ADC with minimum sampling rate $(2\text{–}3)\Omega_{max} \approx 3\omega_{Dm}$.

To extract the wind direction the mean frequency ω_D of $B_s(t)$ must be calculated by the time series within the resolution cell

$$\bar{\omega}_B = \Omega(\omega_0) - \bar{\omega}_D, \tag{3}$$

where $\bar{\omega}_D$ is the mean Doppler shift. At known $\Omega(\omega_0)$ and $\omega_{cw} > \omega_{LO}$ (or $\omega_{cw} < \omega_{LO}$) the value and the sign of ω_D are determined without a quadrature channel.

The chirp in the emitted pulse is excluded using a similar procedure, as in Ref. 8. The signal output by the PD-3 photomixer $A_p(t) = a_p(t)\cos[\omega_0 + \Delta\omega_e(t)]t$, where $a_p(t)$ is the pulse envelope, $\Delta\omega_e(t)$ is the chirp history, is detected through the multiplexer using the same reference oscillation $A_v(t)$. The detected signal

$$A_{p0}(t) = a_p(t)\cos[\Omega(\omega_0) + \Delta\omega_e(t)]t \tag{4}$$

does not depend on the fluctuating reference frequency ω_0. At a given $\Omega(\omega_0)$ the mean chirp $\Delta\bar{\omega}_e$ over the pulse may be calculated. In a first-order approximation it may be subtracted from the mean frequency of $B_s(t)$, where $\Delta\bar{\omega}_e$ enters as an additional term.

As seen, all the necessary parameters as ω_0, $\Omega(\omega_0)$ and $\Delta\omega_e(t)$ are stored in the lidar processor just after the end of the emitted pulse. The full Doppler spectrum may be extracted now by the signal $B_s(t)$, within each gating cell taking into account the parameters of ω_0, $\Omega(\omega_0)$ and $\Delta\omega_e(t)$, and neglecting the LO frequency instability during the lidar return.

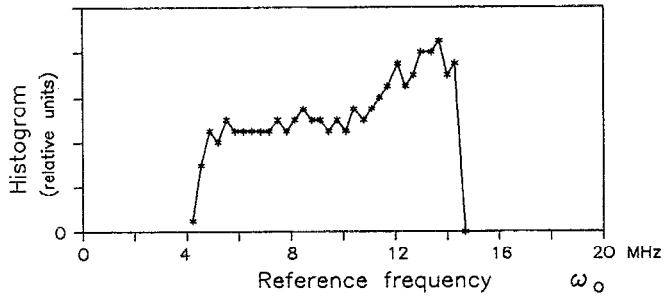

FIG. 4. Histogram of the frequency fluctuations of ω_0 of the tested signal, used in the investigation of the Doppler detector.

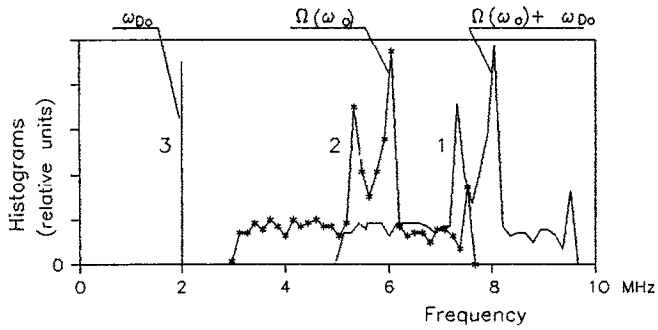

FIG. 5. Histograms of the frequency fluctuations in different parts of the Doppler detector at fluctuating ω_0, according to the histogram on Fig. 4, when a single Doppler line of frequency ω_{D0} is detected: 1—histogram of the frequency $\Omega(\omega_0)+\omega_{Do}$ of the output Doppler signal $B_s(t)$; 2—histogram of the frequency difference $\Omega(\omega_0)$, identical with the histogram 1 and shifted by the input Doppler frequency ω_{Do}; 3—the frequency ω_{Do} of the output processed Doppler signal.

III. TESTING

The Doppler detector (Fig. 1) was tested using a Doppler imitation block with two output signals: (1) the reference signal of frequency ω_0, sweeping within the range 4–15 MHz, so that the frequency $\omega_v(\omega_0)$ was swept within 9–19 MHz (Fig. 2), $\Omega_{min}=3.6$ MHz, $\Omega_{max}=6.4$ MHz; (2) the Doppler signal of frequency $\omega_0+\omega_D$, where ω_D was swept independently around the frequency ω_0.

The histogram of fluctuations of the reference frequency ω_0 within the range $\Delta\omega_0$ is shown in Fig. 4. Two types of Doppler signals were investigated: a single Doppler line of frequency ω_{Do} and a narrow-band Doppler spectrum. The case of a single Doppler line is shown in Fig. 5, which shows the histograms of the frequency $\Omega(\omega_0)+\omega_{Do}$ of the output signal $B_s(t)$ and the frequency difference $\Omega(\omega_0)$ when ω_0 fluctuates as in Fig. 4. The two histograms are identical and separated by the Doppler frequency ω_{Do}. The output Doppler line, shown in Fig. 5, is detected without any distortions. The retrieving of an input Doppler spectrum $B_{in}(\omega)$ [Fig. 6(a)] is demonstrated by the identical output spectrum $B_{out}(\omega)$ [Fig. 6(b)].

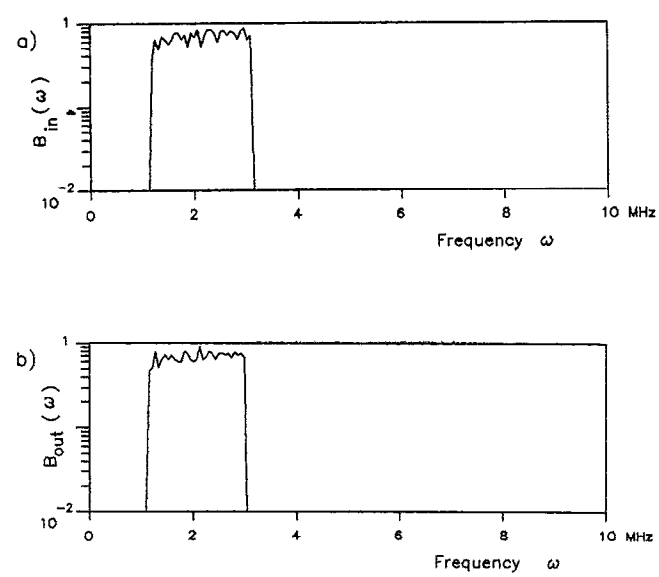

FIG. 6. Extraction of Doppler spectrum: (a) input Doppler spectrum, (b) output Doppler spectrum.

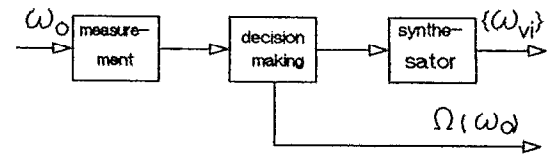

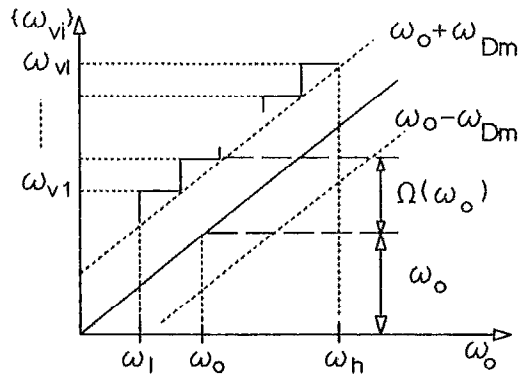

FIG. 7. The use of frequency synthesis for Doppler detection in wide fluctuation bandwidth $\Delta\omega_0$: (a) block schematic, (b) the stepwise tracking frequency $\omega_{vi}(\omega_0)$.

IV. DISCUSSION

As shown, the full input Doppler spectrum can be extracted very precisely at the random fluctuations of the reference frequency within a wide bandwidth $\Delta\omega_0>10$ MHz, using only a single ADC of a reasonable sampling rate. The bandwidth $\Delta\omega_0$ defines the stability tolerance of the laser transmitter. It may be reduced more than 100 times to the order of 10^{-7} and thus low cost laser transmitters may be applied.

In airborne lidars the resultant frequency $\omega_0+\omega_a$, where ω_a is the Doppler shift, caused by the aircraft motion and beam scanning, have to be tracked [$\omega_a\approx 60$ MHz (Ref. 3)]. The tuning of VCO is easily provided in such a wide range, because it is not necessary to strictly track the resultant frequency. The VCO frequency difference from the reference frequency and additional Doppler shift may be taken into account by the known difference frequency $\Omega(\omega_0)$. For comparison, the wide-band tuning of the coherent oscillator (COHO), used as a reference source in Doppler lidars,[1–3] is a serious problem.[3]

Further, a new general approach to the use of the method could be developed to increase the tolerable bandwidth $\Delta\omega_0$ of the variations of ω_0 (or $\omega_0+\omega_a$) above 100

MHz. The reference frequency ω_0 may be measured (before the laser pulse) and then, according to the condition $\omega_v(\omega_0) = \omega_0 + \Omega(\omega_0)$, $\Omega(\omega_0) > \omega_{\mathrm{Dm}}$ a decision is made to generate one of the frequencies ω_{vi} of the previously determined set $\{\omega_{vi}\}$, $i = 1..I$ with the given frequency differences $\Omega(\omega_0)$ [Fig. 7(a)]. The function $\omega_{vi}(\omega_0)$ is of stepwise type [Fig. 7(b)] and may be easily created by a frequency synthesis. It is evident that in this case the use of tuned heterodyne is not necessary. The tolerable laser stability will be reduced to the order of 10^{-6}. Doppler lidar transmitters of 10^{-7}–10^{-6} relative stability may be easily realized, by simple, low cost stabilization technique holding the low-frequency edge ω_1 to the order of $3\Omega_{\min}$. Finally, the technique described here may in principle be applied with minimal modification to other Doppler lidar configurations such as in Ref. 3, which incorporates an injection-seeded TE-CO_2 transmitter.

[1] E. McCaul, H. Bluestein, and R. Doviak, Appl. Opt. **25**, 698 (1986).

[2] R. Schwiesow, A. J. Weinheimer, and V. M. Glover, Proceedings of the 5th Conference on Coherent Laser Radar, Munich, Germany, June 1989, pp. 31–34.

[3] Ch. Werner, P. Flamant, F. Köpp, C. Loth, H. Herrmann, J. Wildenauer, A. Dolfi-Bouteyre, and G. Ancellet; An Advanced Wind Infrared Doppler Lidar for Mesoscale Meteorological Studies, Report Phase O/A-Study, DLR-CNES, December 20, 1989.

[4] B. Bratanov and D. Stoyanov, Proceedings of the Anniversary Session of Radio, Technical University, May 1990, Sofia, Bulgaria (in press).

[5] D. Stoyanov, B. Bratanov, and M. Angelova, Compt. Rend. Bulg. Acad. Sci. **44**, No. 2 (1991), pp. 25–28.

[6] J.-L. Lachambre, P. Lavigne, M. Verreault, and G. Otis, IEEE J. Quantum Electron. **QE-14**, 170 (1978).

[7] P. W. Pace and J. M. Cruinckshank, IEEE J. Quantum Electron. **QE-16**, 937 (1980).

[8] D. Stoyanov, B. Bratanov, and M. Angelova, Sixth International School on Quantum Electronics, 14–19 September, 1990, Varna, Bulgaria (in press).